Antimicrobial, starch based barrier coatings prepared using mixed silver/sodium exchanged bentonite

CLEGG, Francis <http://orcid.org/0000-0002-9566-5739>, BREEN, Christopher <http://orcid.org/0000-0002-5637-9182>, MURANYI, P and SCHÖNWEITZ, C

Published version

CLEGG, Francis, BREEN, Christopher, MURANYI, P and SCHÖNWEITZ, C (2019). Antimicrobial, starch based barrier coatings prepared using mixed silver/sodium exchanged bentonite. Applied Clay Science, 179, p. 105144.

Antimicrobial, starch based barrier coatings prepared using mixed silver/sodium exchanged bentonite.

Francis Clegg[1]*, Chris Breen[1], Peter Muranyi[2], Claudia Schönweitz[2]

[1]Materials and Engineering Research Institute, Sheffield Hallam University, City Campus, Howard Street, Sheffield, S1 1WB, U.K.
[2]Fraunhofer Institute for Process Engineering and Packaging, Giggenhauser Straße 35, 85354 Freising, Germany.

CORRESPONDING AUTHOR: Francis Clegg, E-mail: f.clegg@shu.ac.uk, Tel +44 (0)114 2253062, Fax: +44 (0)114 2253501.

Abstract

The effect of silver nitrate concentration, pre-washed bentonite (to remove extraneous salt) and back-exchange procedures have been explored to assess the type of silver species formed and their behaviour upon exposure to further salts. X-ray fluorescence was used to quantify the amount of silver present and whether in cation exchange sites, whereas X-ray diffraction and transmission electron microscopy identified the silver compounds present.

A further objective was to assess the antimicrobial, barrier and dispersion properties of the silver/sodium bentonites when incorporated into a starch-plasticiser-clay coating used for packaging. The silver/sodium bentonites demonstrated very strong antimicrobial activity towards *Escherichia coli*, *Kocuria rhizophila* and *Aspergillus niger*. Incorporating just 0.03 wt% of silver/sodium bentonite in the coating (0.2 µmol/m^2 Ag in dried coating with thickness of 14 µm) produced a >4.4 log reduction against an initial loading of 2.1 x 10^5 CFU/object for *E. coli*. Water vapour barrier properties of coatings prepared on paper and containing the mixed silver/sodium bentonite were unaffected since water vapour transmission rate values of ~20-40 g/m^2.day (23°C, 50% relative humidity) were maintained. Also the presence of silver did not adversely affect the clay dispersion or the barrier

properties. The Ag^+ release profile from mixed silver/sodium clay upon addition of HNO_3 and $NaNO_3$ is discussed.

Keywords: layered silicate, silver complexes, antimicrobial activity, barrier coatings.

1. Introduction

Current estimates indicate that the growth and production of food requires 9 GJ of energy per individual each year (Johansson *et al*., 2012). Consequently, it is imperative that as much food as possible is consumed and wastage minimised. Barrier packaging has a critical role to play in prolonging the shelf life of food by controlling the movement of water and oxygen to the packaged product. It is also critically important to minimize microbial and fungal attack of both the food product and the package which protects it.

The incorporation of high aspect ratio Na-bentonite into starch plasticiser coatings can significantly reduce the water vapour barrier properties of the base paper (Johansson *et al.*, 2012, Olsson *et al*. 2014a,b), which relies on a maximum dispersion of the platelets in the water based coating. The bentonite is also an ideal substrate from which to incorporate and control the release of antimicrobials.

Silver is a potent antimicrobial with renewed interest because of its wide applicability and the need to control infectious diseases, in hospitals and other communal environments, that are becoming resistant to current antimicrobial treatments (Rai, *et al*., 2012). Silver oxide (Ag_2O), silver chloride (AgCl) and silver nitrate ($AgNO_3$), have been investigated (Sedlarik et al., 2010) and more recently silver nanoparticles have been targeted due to their enhanced properties at the nano-scale (Tolaymat *et al*., 2010). Silver species have been evaluated for;

wastewater treatment (Mthombeni *et al*., 2012), coatings in medical devices (Schierholz *et al*., 1999), dental resins (Herrera *et al*. 2001), burn wound dressing (Jones *et al*., 2004) and consumer products (e.g. sportswear, refrigerators) (Moretro and Langsrud, 2011). The use of silver-containing clay in packaging applications remains largely unexplored (Busolo and Lagaron, 2013; Benhacine *et al*., 2016).

The preparation of silver nanoparticles involves initial reduction of silver cations using chemicals (e.g. glucose or $NaBH_4$) (Shameli *et al*., 2010a; Miyoshi *et al*., 2010), UV or gamma radiation (Huang and Yang, 2008) or heating (Waterhouse *et al*., 2001). To prevent agglomeration they must be stabilised by surfactants (Pal *et al*., 1998), polymers (Dong *et al*., 2007), chemical stabilisers (Yonezawa *et al*., 2000) or solid inorganic substrates such as activated carbon (Yoon *et al*., 2008), zeolites (Top and Ulku, 2004; Yang *et al*., 2008), TiO_2 (Nikolov *et al*., 2010) and $Al(OH)_3$ (Seo *et al*., 2012). The large surface areas of clays together with their cation exchange properties make them particularly useful as a substrate (Varadwaj and Parida, 2013). Individual Ag^+-ions occupying exchange sites may act as the nucleus for nanoparticle growth as more and more Ag^+ cations are adsorbed onto these individual Ag^+-ions to form Ag agglomerates (Tokarsky *et al*., 2010). The main emphasis in the literature is on the production of silver nanoparticles on clay surfaces rather than clays with individual silver ions occupying the exchange sites, though Busolo and Lagaron (2013) describe an ionic silver exchanged montmorillonite in the absence of silver nanoparticles. Others describe montmorillonite systems which contain silver ions and metallic silver nanoparticles with Ag_2O or AgOH at the surface (Keller-Besrest *et al*., 1995; Magana *et al*., 2008).

A number of clays and clay minerals have been used as substrates for silver nanoparticles. Following an earlier report on the formation of Ag-nanoparticles on kaolin (Patakfalvi and Dekany, 2004), Shameli *et al.* (2010a) used chemical reduction in the presence of talc and UV radiation with montmorillonite (Shameli *et al*., 2010b). Others have used vermiculite (Valaskova *et al*., 2010), palygorskite (Zhao *et al*., 2006), fluoromica (Dizman *et al*., 2007) and Laponite® (Huang and Yang, 2008). Patel *et al*., (2009) used selected alkylammonium modified clays to localise silver ions at the clay surface followed by reduction to form silver nanoparticles, whereas Roy *et al*. (2017) was able to deposit reduced-sized silver nanoparticles on the surface of acid activated montmorillonite in the absence of reducing agents. The high aqueous solubility of silver nitrate ($AgNO_3$) makes it the preferred source of Ag^+ (Praus *et al*., 2008), although other chemicals, e.g. Ag-2-(4-thiazolyl)benzimidazole, have been used (Ohashi *et al*., 1998).

The antimicrobial effectiveness of silver in its many forms has been proven against a wide variety of microbes (Ohashi *et al*., 1998), specific examples include; *Escherichia coli*, *Staphylococcus aureus*, *Klebsiella pneumonia*, *Enterococcus faecalis*, *Pseudomonas aeruginosa* (Sedlarik *et al*., 2010) *Candida albicans* (Marambio-Jones and Hoek, 2010) and *Salmonella (*Busolo *et al*., 2010). The mechanisms underlying silver's activity have been debated (Sondi and Salopek-Sondi, 2004; Marambio-Jones and Hoek, 2010; Tathdil et al., 2011; Xiu et al., 2012), but the general consensus is that an accumulation of ionic silver within the cell is required. This may result from the transportation of Ag^+ after dissolution through the bacterial cell wall or after silver nanoparticles penetrate the cell walls and then dissolve. Silver clay is itself an ionic species and so potentially provides an antimicrobial surface. Indeed, electrostatic forces may attract negatively charged bacterial membranes to clay surfaces wherein the positively-charged silver ions kill the microorganisms or render

them unable to replicate (Magana *et al*., 2008). Moreover, silver-ions can be displaced from the clay by incoming cations thus releasing Ag^+ to attack the microbes.

The current concern regarding nanoparticles in the food chain demands a deeper knowledge of the formation of these nanoparticles so that a greater level of control can be achieved. This study therefore takes care to prepare various mixed silver/sodium bentonites and assess the effect of pre-washing to remove extraneous salt, silver loading and back exchanging with Na^+-ions after silver treatment on silver species formed. Extraneous salts are typical in commercial products as a by-product of the clay production process and removing them represents a significant environmental and economic challenge. One aspect of the study was to compare the number of individual Ag^+-ions located at cation exchange sites relative to those forming silver-containing (nano)particles and study the effect of preparation/processing methods on their form. The mixed silver/sodium bentonites prepared were characterised using X-ray diffraction (XRD), X-ray fluorescence (XRF), transmission electron microscopy (TEM) and energy dispersive X-ray analysis (EDAX). Their antimicrobial activity was assessed when applied as a minor component in a recently developed bio-based, barrier coating containing starch, plasticiser and clay (Johansson *et al*., 2012). The clay, Na^+-bentonite, is primarily present as the barrier component within the starch matrix and therefore an ideal substrate/stabilising agent from which to release silver ions and impart antimicrobial activity. The requirement for antimicrobial activity in these coatings is twofold; firstly to protect the components being packaged and secondly to protect the barrier material itself since starch is susceptible to attack by certain microbes; particularly at high relative humidities.

2. Experimental

2.1 Materials

Na-bentonite (Cloisite® Na^+, Southern Clay Products) with cation exchange capacity (CEC) of 92.5 meq/100 g is referred to as Na^+Mt. Starch (S1), received from Cargill (Germany), is derived from waxy corn (98% amylopectin) and is hydrophobically modified and thinned. Starch (S2), sourced from Lyckeby (Sweden), is a hydroxypropylated potato starch (Perlcoat 155). Silver nitrate ($AgNO_3$, ≥99.0%), silver oxide (Ag_2O, 99%), nitric acid (HNO_3, ACS reagent, 70%), sodium chloride (NaCl, ≥99.0%), sodium nitrate ($NaNO_3$, ≥99.0%), sodium hydroxide (NaOH, ≥98.0%) and polyethylene glycol with molecular mass 600 (PEG600, standard grade) were obtained from Aldrich and used without further modification.

2.2 Silver clay preparation

Four different silver clays were prepared using either unwashed or prewashed sodium bentonite (UW-Na^+Mt and PW-Na^+Mt, respectively) and amounts of $AgNO_3$ required to satisfy 20%, 120% and 400% of the CEC of the clay. PW-Na^+Mt was prepared by repeatedly dispersing UW-Na^+Mt in deionised water, followed by agitation and centrifugation until the conductivity of the decanted supernatant was less than 50 μS. After any treatment with silver all samples were thoroughly washed as described in the previous sentence, in order to remove soluble cations not occupying exchange sites. During preparation all samples were covered with aluminium foil to minimise photodecomposition of any silver species present. The silver clays were labelled as PW-Na^+Mt-20%Ag, UW-Na^+Mt-20%Ag, UW-Na^+Mt-120%Ag and UW-Na^+Mt-400%Ag. The percentage number refers to the concentration of Ag^+-ions used to treat the clay as a percentage of the CEC, rather than the actual amount of silver present on the bentonite after the exchange process. To identify whether Ag^+-ions were occupying cation-exchange sites in UW-Na^+Mt-120%Ag it was further backwashed (BW) with aqueous NaCl (10 x CEC) to displace the Ag^+-ions by Na^+-ions and was labelled as UW-

Na^+Mt-120%Ag-BW(NaCl). To aid identification of silver species present on the silver clays and to evaluate changes to silver species upon mixing with various salts, UW-Na^+Mt-120%Ag was also backwashed using NaOH, identified as UW-Na^+Mt-120%Ag-BW(NaOH), $NaNO_3$, identified as UW-Na^+Mt-120%Ag-BW($NaNO_3$), and HNO_3, identified as UW-Na^+Mt120%Ag-BW(HNO_3) using the same procedure and analysed by XRD. All backwashed samples were thoroughly washed with deionised water (as described above) after treatment.

2.3 Starch-plasticiser-clay coatings.

All coatings were prepared using 60 wt% starch, 12 wt% PEG600 and 28 wt% clay. Aqueous starch dispersion was cooked at 95°C for 1 hr then cooled to 60°C before adding PEG600. After mixing for 1 hour, clay was added and mixed for a further 2 hours. The total clay content was always equal to 28 wt%; additions of silver clay at concentrations lower than this value were compensated by the addition of PW-Na^+Mt. The resulting dispersion was double coated (total coat weight ~25g/m^2) on paper and each coating was dried in an oven at 105°C for 1 minute and then 60°C for 4 minutes. The paper, Gerbier HDS, was a sized, coated and calendered flexible packaging paper (50 g/m^2) and supplied by Ahlstrom (Pont Evêque, France). Aliquots of the coating were also dried on 2.5 x 2.5 cm square glass slides at 40°C (equivalent coating weight of 800 g/m^2) and were used for antimicrobial testing.

For comparative purposes silver oxide (Ag_2O) was finely ground using a pestle and mortar and added to the starch/PEG600/PW-Na^+Mt clay coatings.

2.4 Sample characterisation

X-ray diffraction patterns of silver clay powders or starch-PEG600-clay coatings on paper were obtained using a Philips X'Pert Pro diffraction system using a Cu-tube (λ = 1.542 Å), operating at 40 kV and 40 mA. Diffraction data from standards and the library database

were used to identify the silver salts present. XRF analytical data for SiO_2, Al_2O_3 and Na_2O was obtained using a Philips PW2440 sequential spectrometer, using lithium tetraborate fused beads. XRF data for silver, sulphur and chlorine was obtained using pressed pellets. Water vapour transmission rates (WVTR) were obtained using Payne cups containing silica gel and maintained at 23°C and 50% relative humidity. TEM images were obtained using a FEI Tecnai G2 Spirit TEM instrument with an 80 kV accelerating voltage. Samples were prepared by placing a 5 µl drop of dispersed clay mineral (0.005 g/20 ml) on a Formvar/carbon coated 200 mesh TEM grid (Agar Scientific Limited). EDAX of the particles were performed using a FEI Quanta 650 scanning electron microscope (SEM) equipped with an Oxford Instruments X-Max detector.

2.5 Antimicrobial Testing

All micro-organisms were sourced from the German National Resource Centre (DSM), Braunschweig. Non pathogenic strains of *E. coli* (DSM 498) and *K. rhizophila* (DSM 348) were chosen as test micro-organisms, the former is a vegetative bacterium (gram –ve) and often causes food borne diseases, the latter is an airborne bacterium (gram +ve) and has distinct yellow colonies. Fungi *A. niger* (DSM 1957) was also tested, it is a spore former, ubiquitous in the environment (especially soil) and often an initiator of food spoilage causing black mould disease on foodstuffs including grapes, onions, and peanuts. The conidiospores of *A. niger* were also used for the investigations.

Vegetative cells of *E. coli* and *K. rhizophila* were gained from an overnight culture. For this, 100 ml nutrient broths (Merck, Darmstadt, Germany) were inoculated with cell material and incubated for 16-18 h at strain specific temperatures (*E. coli* 37°C, *K. rhizophila* 30°C). Finally, 20 ml cell suspensions were washed twice by centrifugation at 10,000 g for 10 min

and re-suspended in sterile deionized water. The cell concentrations in the suspensions were determined in a counting chamber by microscopic methods. For the conidiospores of *A. niger*, YGC plates (Yeast extract glucose chloramphenicol, Merck, Darmstadt, Germany) were inoculated by plating 0.1 ml suspension of cell material. After an incubation period of 10 days at 30°C, the conidiospores were harvested by tapping the plates with sterile sea sand. For deposition of the sand particles, the agglomerates of sand and spores were suspended in sterile ringer solution treated with ultrasound for 1 min. The supernatant containing the conidiospores was removed and the suspension stored at 4°C. Before usage, the conidiospores were washed twice and re-suspended in sterile deionized water.

Antimicrobial activities of silver clays were tested as starch-plasticiser-clay samples coated on glass or paper according to the Japanese Industrial Standard (JIS Z 2801: 2000), which is a quantitative method for the evaluation of antimicrobial containing products. It involved the preparation of test suspensions with diluted nutrient broth (500-fold, Merck), each of about 2.5 to 10 x 10^5 colony forming units (CFU)/ml. In the case of coated papers, three test pieces (5 x 5 cm) of each sample and test strain were artificially inoculated with 400 µl suspension (number of cells/spores per test piece should be 1.0 to 4.0 x10^5), covered by a sterile PET film (4 x 4 cm, Mitsubishi Polyesters) and finally incubated for 24 hours at 37°C for *E. coli* and 30°C for *K. rhizophila* and *A. niger* at 90% relative humidity. For the trials with the glass slides (2.5 x 2.5 cm), the samples were inoculated with 200 µl test suspension and covered with a PET film of 2 x 2 cm. After storage, each test piece was transferred into a sterile stomacher pouch with 100 ml sterile Ringer solution (Oxoid), and rubbed for 1 min. The viable count was determined by microbiological methods and referenced against the final count of the initial load. The result is expressed as a microbial log reduction.

2.6 Leaching experiments

An aqueous dispersion (30 ml) containing 0.33 wt% PW-Na^+Mt-20%Ag was offered increasing amounts of HNO_3 or $NaNO_3$ and mixed for 24 hours. The dispersions were centrifuged and the supernatants analysed for the presence of Ag ions by ICP-OES (HORIBA Jobin Yvon - Activa). Calibration standards were prepared using certified Ag standards (Aldrich) and dilute HNO_3 was added to the supernatants to prevent Ag^+-ions from precipitating. All samples were prepared using amber plastic bottles to prevent photo-decomposition.

3 Results

3.1 Silver Clay Characterisation

Table 1 presents the XRF data obtained from the different silver/sodium bentonites; the top section identifies their weight percentage oxide levels, whereas the bottom section provides the percentage of Ag or Na present (after preparation) relative to 100% of the CEC. The XRF analysis showed that prewashing Na^+Mt reduced the Na_2O content from 3.18 wt% (i.e. UW-Na^+Mt) to 2.66 wt% (i.e. PW-Na^+Mt) and also completely removed sulphur and chlorine, which confirms that the extensive washing procedures served to remove the excess salt and sodium cations not occupying exchange sites. The amount of Na_2O (2.66 wt%) in the PW-Na^+Mt more accurately reflects the CEC of UW-Na^+Mt reported by the manufacturers to be 92.5 meq/100g.

The PW-Na^+Mt-20%Ag sample contained more Ag^+ and less Na^+ when compared to PW-Na^+Mt demonstrating that a portion of exchangeable Na^+ had been replaced by Ag^+.

The UW-Na^+Mt-20%Ag sample also showed an equivalent reduction in Na_2O content compared to PW-Na^+Mt-20%Ag, but this unwashed sample retained more silver (11.7 % of

the CEC compared to 7.0% of the CEC). The UW-Na^+Mt-120%Ag and UW-Na^+Mt-400%Ag samples exhibited commensurately higher silver and lower sodium contents than those in either PW-Na^+Mt-20%Ag or UW-Na^+Mt-20%AgC. These values for the clays with high silver loadings suggest both higher numbers of silver cations on exchange sites (confirmed by lower sodium values), together with an increased quantity of insoluble silver complexes because the combined amounts of Ag and Na are greater than that required to fulfil 100% of the CEC (bottom section of Table 1).

The values for UW-Na^+Mt-120%Ag-BW(NaCl) showed that backwashing UW-Na^+Mt-120%Ag with NaCl slightly reduced the amount of silver and increased the quantity of sodium to near that of PW-Na^+Mt. This confirms that the sodium ions initially replaced by silver ions could be back-exchanged. Relatively less silver ions removed compared to sodium ions back-exchanged were observed since any silver released would react with chlorine ions to produce the sparingly soluble AgCl (as discussed below), which remained in the sample.

XRD analysis of the residue collected after evaporating water from the supernatant of a washed and centrifuged Na^+Mt dispersion clearly indicated the presence of both NaCl and $NaSO_4$. Sulphur was detected at only very low amounts in the silver-clays treated with relatively high concentrations of Ag^+ (i.e. at 120% and 400%), whereas chlorine remained in those prepared using UW-Na^+Mt. The amount of chlorine increased as the amount of $AgNO_3$ offered was increased but did not surpass that of the unwashed Na-clay. The one exception was UW-Na^+Mt-120%Ag-BW(NaCl) where the chloride content of 1.07 wt% demonstrated that the introduction of chloride during the backwashing process caused the formation of additional insoluble chloride complexes.

The most significant observation in the XRD patterns of different silver/sodium clays was that PW-Na^+Mt-20%Ag did not show any additional reflections when compared with that of

UW-Na^+Mt (Figure 1a and 1b, respectively). The presence of reflections at 32.2, 46.1, 54.8 and 57.4 °2θ confirmed the presence of silver chloride (AgCl) in all the other silver/sodium clays (Figure 1c-e) and their intensities in the different samples corresponded with the concentrations of chlorine determined by XRF (Table 1). The 060 reflection of the clay at 62.0 °2θ can be used as an internal standard to relate the relative intensity of reflections due to the silver species within each silver/sodium clay.

The reaction of $AgNO_3$ with NaCl present in the UW-Na^+Mt logically led to the formation of sparingly soluble AgCl. XRD analysis of UW-Na^+Mt-20%Ag indicated that only AgCl was present in addition to clay, but several minor reflections positioned at 31.2, 32.6, 33.8, 37.2, 39.6 and 47.4 °2θ in the XRD trace of UW-Na^+Mt-120%Ag confirm the presence of additional species. These reflections were not unequivocally assigned due to their low intensity (representing low amounts) but the reflections at 31.2, 33.8, 37.2 and 47.4 °2θ do closely match those of silver sulphate (Ag_2SO_4), which reflects the low amount of sulphur detected by XRF (Table 1). No reflections are present representing silver sulphide (Ag_2S), a species known to result from the reaction of atmospheric hydrogen sulphide (H_2S) with metallic silver (as in the tarnishing of silver) so the source of sulphur is likely to be from extraneous $NaSO_4$ salt present in the UW-Na^+Mt even though a very high proportion was removed during the preparation and washing process. The small shoulder at 32.6 °2θ, reflection at 33.8 and possible reflection at 39.6 °2θ could suggest the presence of silver carbonate (Ag_2CO_3), the CO_3 of which could feasibly derive from a mineral carbonate present as a contaminant in the bentonite (in support thermogravimetric-mass spectroscopy does detect the presence of CO_2 as it is heated between 350 and 500°C). The XRD trace of UW-Na^+Mt-400%Ag is similar to that of UW-Na^+Mt-120%Ag, but the former contains a broader reflection at 32.2 °2θ and more intense reflections at 33.8 and 39.6 °2θ, it is believed that

these changes are due to both an increase in the amount of Ag_2CO_3 (also supported by a more prominent reflection at 18.5 °2θ – data not shown) and also the presence of AgO. Given the intensity of the AgCl reflections in the diffraction traces of UW-Na^+Mt-120%Ag and UW-Na^+Mt-400%Ag are very similar, the AgO is presumed to derive from the increased amount of $AgNO_3$ used in the preparation via the possible formation of metallic silver even though in this particular sample there is no strong evidence of this latter species.

The backwashing of UW-Na^+Mt-120%Ag with $NaNO_3$ or NaCl results in the Ag_2SO_4 remaining (Figure 2 - note characteristic reflection at 31.2 °2θ) and the formation of metallic silver as evidenced by the reflection at 38.2 °2θ. For both these clays metallic silver presumably results from the photodecomposition of AgCl occurring during the additional processing. A decrease in the amount of AgCl is observed when backwashing with $NaNO_3$, perhaps supporting its conversion to metallic silver whilst an increase in AgCl with UW-Na^+Mt-120%Ag-BW(NaCl) is due to the formation of any soluble Ag^+ ions removed from cation-exchange sites combining with Cl^- ions to form AgCl, which is driven by its very low solubility. Note to allow a more detailed comparison of the smaller reflections the upper section of the diffraction trace from UW-Na^+Mt-120%Ag-BW(NaCl) has been omitted. The intensity of the reflection at 32.2 °2θ is six times greater than that from UW-Na^+Mt-120%Ag.

When UW-Na^+Mt-120%Ag is backwashed with HNO_3 the removal of all reflections occurs apart from those due to AgCl, which is due to the solubilisation of silver carbonates and sulphates. A dramatic change occurs when UW-Na^+Mt-120%Ag is backwashed with NaOH; the removal of AgCl occurs and several more intense reflections are observed. The reaction of AgCl with NaOH is not anticipated to occur in the absence of a base so the clay (or other species present) must play a role in its dissolution and conversion to other species. The distinctive reflections at 18.5 (data not shown) and 33.8 °2θ strongly support the presence

of Ag_2CO_3, whereas the distinctive reflection at 34.1 °2θ indicates the presence of AgO. Ag_2O is also a likely species to be present, but its characteristic reflections overlap those of Ag_2CO_3, AgO and metallic Ag and so any confirmation is not possible. The presence of metallic silver is likely due to the relatively intense and broad reflection at 38.2 °2θ associated with that at 44.3 °2θ.

Although XRD was unable to identify silver particles on the PW-Na^+Mt-20%Ag sample, further examination by TEM did confirm a small fraction was present (Figure 3). The majority of clay mineral platelets showed no evidence of silver particles (Figure 3A). However, when present they did appear as either very thin (as indicated by their lighter contrast), circular/oblong shapes closely integrated with the clay layer structure (Figure 3B) or as distinct and separate particle identities (Figure 3C, 3D and 3E). The thin, closely integrated silver species were common, ranged from approximately 2-40 nm in diameter and could derive from clusters of silver atoms generated around cation exchange sites as discussed by Tokarsky *et al*., (2010) or alternatively, by the reduction of silver ions in solution and then precipitation on to the clay surface. The distinct and separate particles were much darker in contrast, appeared to be positioned on top or to one side of the clay platelets and tended to form larger clusters, some up to 700 nm (Figure 3D).

EDAX combined with SEM showed that approximately half of the darker particles did contain silver and a small fraction of these also contained either chlorine or sulphur indicating the presence of AgCl and $AgSO_4$, respectively - thus indicating the extensive washing procedures employed did not eliminate all the sodium chloride or sodium sulphate. The remaining silver containing particles indicate the possible presence of Ag_2CO_3, AgO, Ag_2O or similar species. Although oxygen and carbon were detected, equivocal distinction could not be made since the oxygen may arise from neighbouring clay mineral due to the

large interaction volume of electrons whilst carbon would be detected from the conducting carbon coating used to alleviate charging effects during the analysis. A very small number of angular, crystalline particles were observed (Figure 3e) and closely resemble those confirmed as metallic silver particles using high resolution TEM and X-ray diffraction (Miyoshi *et al*., 2010).

In general the distinct and separate silver particles were more densely populated, relative to the clay platelets, within the corners of the TEM grids (Figure 3C). This was considered likely to occur during the preparation of the TEM sample when the dispersion droplet shrinks through evaporation and pulls the silver particles to the grid corners where they are constrained, consequently the TEM images obtained at the corners of the grids may report an erroneously increased quantity of dark silver particles relative to clay mineral. The particles that did not contain silver, as evidenced by EDAX combined with SEM and were presumably due to mineral impurities in the clay – indeed a small portion contained high quantities of magnesium and calcium supporting the presence of carbonate minerals.

These TEM images demonstrate that the XRD technique was not sensitive enough to detect the small number of silver particles in PW-Na^{+}Mt-20%Ag. If the XRF data is considered accurate then the difference relating to the decrease in percentage of Na, i.e. a decrease of -5.3% relative to 100% of the CEC (Table 1, bottom section), could account for the Ag^{+}-ions being located within cation exchange sites. Whereas, the corresponding +1.7% difference in the same sample for silver above that of the CEC could account for the silver present in the discreet separate dark particles. An alternative scenario, or in addition to, may be that the thin integrated circular/oblong discs are derived from silver-exchanged sites that initiated their growth. Unfortunately, single Ag^{+}-ions could not be imaged due to the resolution of the specific TEM utilised, however an agglomeration of Ag^{+}-ions at a cation exchange site

could. All the features observed in the PW-Na^+Mt-20%Ag sample were also observed in the UW-Na^+Mt-120%Ag sample. However, a much higher density of the darker distinct and separate particles were observed showing a higher presence of the silver containing species, which reflects the XRD data (Figure 1).

3.2 Antimicrobial Activity Tests

XRF analysis of the starch showed no anions were present that could react with the silver species on the clay. XRD analysis also indicated no additional silver species were removed or created during the mixing with starch (data not shown). The first screening test demonstrated that after 24 hours incubation all the silver-clays, at 5.7 wt% loading in a starch (S1)/PEG600/clay coating, showed a positive and significant antimicrobial activity towards *E. coli* since a >3.3 log reduction was observed against an initial load of 1.2 x 10^5 CFU/object (Figure 4A). The reference and control (i.e. containing only UW-Na^+Mt) both showed a >1.0 log increase demonstrating that UW-Na^+Mt, starch or PEG600 had no antimicrobial activity against *E. coli*.

The efficacy, or lowest-observed-effect-level, of the PW-Na^+Mt-20%Ag against *E. coli* was assessed using the starch (S1)/PEG600/clay coating in three separate trials, each trial containing lower amounts of clay (Figure 5A-C, respectively). Direct comparison between trials was not considered possible due to different initial loadings, i.e. ~1 x 10^{-6} for Figure 5B and ~1 x 10^{-5} for Figures 5A and 5C, which could influence the efficacy of the system. However, to aid comparison and compensate, samples with the same concentration of PW-Na^+Mt-20%Ag were utilised in subsequent trials. With only 0.03 wt% of PW-Na^+Mt-20%Ag a >4.4 log reduction was observed, but since all samples showed a similar, significant and positive antimicrobial activity the ultimate efficacy was not determined.

The antimicrobial activity of 0.28 wt% PW-Na^+Mt-20%Ag, when incorporated in the starch (S1)/PEG600/PW-Na^+Mt coating on glass slides, showed a significant effect when assessed against conidiospores of *A. niger*. A >2.9 log reduction was observed against an initial loading of 5.9 x 10^3 CFU/object (Figure 4B). The antimicrobial activity of the UW-Na^+Mt-400%Ag, in the potato starch (S2)/PEG600/PW-Na^+Mt coating (~10 µm thickness) on paper was tested against *K. rhizophila*. A decrease in activity occurred as the Ag-clay loading decreased from 4.3 to 2.9 and then to 1.4 wt% (>4.7, >2.6 and >1.5 log reduction, respectively) indicating the level of efficacy for UW-Na^+Mt-400%Ag and bacteria (Figure 4C). Given that Ag_2O is a likely candidate to be present in silver clays and it can be used as an antimicrobial agent its activity was tested against *E. coli* when dispersed in starch (S1)/PEG600/PW-Na^+Mt films coated on glass slides. Figure 6 shows that >4.4 log reductions were observed with an initial loading of 2.1 x 10^5 CFU/object, when 0.05, 0.10, 0.19 or 0.38 wt% Ag_2O was incorporated into the coating containing PW-Na^+Mt. Based on the amount of elemental silver present, the amount of Ag_2O added was equivalent to adding 5, 9, 17 and 35 wt% PW-Na^+Mt-20%Ag, respectively. Although the results showed that Ag_2O also exhibited a strong antimicrobial activity against *E. coli*, differentiation between the effectiveness of silver clay or silver oxide could not be established using the concentrations and testing procedures studied herein.

3.3 Leaching Experiments

The percentage of Ag ions leached into aqueous solution from PW-Na^+Mt-20%Ag increased with increasing concentrations of HNO_3 or $NaNO_3$ (Figure 7). When 3.18 x 10^{-4} mol L^{-1} of HNO_3 or $NaNO_3$ was offered (first data point in Figure 7) to PW-Na^+Mt-20%Ag then a similar amount of Ag^+-ions was released, 5.62 x 10^{-5} and 7.25 x 10^{-5} mol L^{-1}, respectively. HNO_3 was

more able to entice Ag^+-ions from the clay and much higher amounts of Ag were released compared to when $NaNO_3$ was added. When 6.35 x 10^{-4} mol L^{-1} HNO_3 was added 4.26 x 10^{-4} mol L^{-1} Ag was removed, whereas with $NaNO_3$ only 2.77 x 10^{-4} mol L^{-1} Ag was removed.

3.4 WVTR and Silver Clay Dispersion

The WVTR value for the uncoated base paper was 780 g/m^2.day and this was reduced to 321 g/m^2.day (indicating a better vapour barrier) when a starch coating was applied. Incorporating UW-Na^+Mt and PEG600 reduced the WVTR values by a factor of ten to 22 g/m^2.day (Figure 8). The WVTR values of starch (S1)/PEG600/PW-Na^+Mt coatings prepared on paper and containing the different silver-clays (at a loading of 5.7 wt%) increased slightly to 25-33 g/m^2.day compared with the coating containing UW-Na^+Mt alone, whereas that for a coating containing 28.6 wt% UW-Na^+Mt-120%Ag-BW(NaCl) increased to 39.7 g/m^2.day – encouragingly these small changes are considered insignificant.

XRD demonstrated that all the silver clays dispersed to the same extent as UW-Na^+Mt; the example in Figure 9 shows that the dispersion of UW-Na^+Mt in S1 and PEG600 was very similar to that containing PW-Na^+Mt-20%Ag since their d_{001} spacings both increased from ~13.0 Å (6.78 °2θ) to 18.2 Å (4.86 °2θ). The higher order 00l reflections exhibited by the clays in both coatings were clearly observed indicating the clay layers, which were present as stacks and intercalated with starch and PEG600 were highly ordered.

4. Discussion

The complex reactivity of silver species and their low aqueous solubility made preparation of pure Ag-exchanged clay very challenging. The presence of extraneous salts in the as-received clay contributes to the complexity since they react with silver cations, cause

precipitation and lead to silver nanoparticles. XRF and XRD (Table 1, Figure 1) demonstrated that UW-Na^+Mt contained NaCl and $NaSO_4$ and confirmed that AgCl present in the sodium-silver clays arose from the reaction of NaCl with Ag^+. The low amounts of sulphur detected in any sodium-silver clay and the low intensity reflections for Ag_2SO_4 indicated only minimal amounts of this salt could be formed from the reaction of $NaSO_4$ with Ag^+. If more was initially formed then this relatively soluble species could have been removed during washing. In general, the presence of any halide or other anion (e.g. carbonate) needs to be considered when preparing Ag-exchanged clay to avoid precipitation of Ag-(nano)particles. Production of pure Ag-exchanged clay was not possible using the methodology herein, though TEM (Figure 3), XRD (Figure 1) and XRF data (Table 1) indicated significantly fewer insoluble silver species were created when using PW-Na^+Mt. Ag-(nano)-particles were produced even when the low amount of $AgNO_3$ used to treat PW-Na^+Mt, i.e. 20% CEC, was specifically chosen to target ion-exchange onto the most energetically favourable sites and result in increased distances between exchanged silver cations thereby minimising their potential to agglomerate. The presence of Ag_2CO_3 and Ag_2SO_4 on UW-Na^+Mt-120%Ag and UW-Na^+Mt-400%Ag coincided with the use of larger quantities of $AgNO_3$. Presumably, when Cl^- was fully consumed in forming AgCl, the remaining $AgNO_3$, not participating in cation-exchange, was transformed into these salts. Sohrabnezhad *et al*. (2015) also showed that reduction of $AgNO_3$ by ethylene glycol in the presence of montmorillonite and Na_2CO_3 did indeed form Ag_2CO_3. TEM showed that some metallic silver particles were evident, which could derive from the reaction of silver halide or silver nitrate (though much less photosensitive) with photons or reducing agents (Shameli *et al*., 2010a).

For microbes to be killed during an antimicrobial test, Ag^+ must leach from the silver clay at a sufficient rate, enter the nutrient medium and then interact. Any Ag^+-ions leached from

exchange sites must be replaced by incoming cations from the salts within the nutrient medium. In application ingress of cations would result from contact with the packaged material or external sources. Once Ag^+ ions on the clay had been fully utilised any Ag^+ ions present would arise from the constrained dissolution of Ag_2CO_3, Ag_2SO_4 or AgCl.

The antimicrobial activity of all silver clays was positive against *E. coli* (Figure 3A) when present at 5.7 wt% loading within a starch (S1)/plasticiser/PW-Na^+Mt matrix. PW-Na^+Mt-20%Ag also produced a >4.4 log reduction against an initial loading of 2.13 x 10^5 CFU/object when dispersed at 0.1 wt% loading (or 0.03 wt% of the total starch/plasticiser/clay content). This equates to 14.4 nano-mol of Ag^+ per gram of dried coating or 0.2 µmol Ag^+ per m^2 of dried coating with a thickness of 14 µm, i.e. a coating thickness that results in a WVTR value of ~20 g/m^2.day. The true efficacy of silver clay was not established herein and lower loadings may provide the same positive effect. However, a balance between the lowest amount necessary to instantly kill microbes in the packaged material and that required to provide a sustained release against subsequent cohorts arriving (e.g. by airborne routes) needs consideration.

All silver clays contained more than one silver species, thus preventing an assessment of their individual antimicrobial activity in the presence of clay. Ag_2O was investigated independently and found to be effective (Figure 5) even though the particle size used is likely to be much larger than that formed on the clay and potentially less reactive. With the example of UW-Na^+Mt-120%Ag-BW(NaCl)), it is interesting to note that given the low solubility's of the species present (AgCl, Ag_2SO_4 and metallic silver) the low amounts available via dissolution are still sufficient to act against microbes.

The amount of Ag^+-ions released from PW-Na^+Mt-20%Ag in the presence of increasing concentrations of HNO_3 (which is considered an aggressive food simulant) or $NaNO_3$ was

highest with the former; since the protons are able to displace silver cations from exchange sites (to produce proton exchanged clay) as well as react with Ag_2O or metallic silver (to produce $AgNO_3$ (aq)). With $NaNO_3$, the only credible source of Ag^+-ions in solution is via their displacement from exchange sites. The fact that silver ions are leached during the treatment with $NaNO_3$ provides further support that Ag^+ occupies exchange sites on the clay.

Busolo *et al.* (2010) also monitored Ag^+ release from silver-treated clay (3.4% Ag) containing metallic silver nanoparticles and dispersed in PLA into HNO_3 solution. The release of Ag^+ was very low during the first 6 days, but increased significantly in an exponential fashion after 8 days, when the hydrolysis of PLA became extensive. Benhacine *et al*. (2016) also studied the release of Ag^+ from silver nanoparticles formed on montmorillonite and dispersed in PCL using similar methodology, they state that the release was dominated by silver nanoparticles at the surface of the films before 12 days and that release was mainly limited by diffusion.

Despite production of pure silver-exchanged clay being unobtainable, clay containing a range of silver species could be beneficial in antimicrobial applications. The exchanged silver cations may offer an initial burst of activity to provide a quick kill upon initial contact, whereas the inherently low solubility of silver-containing particles may offer a method of sustained release. The potential replenishment of silver cations on exchange sites by those released by dissolution of solid silver nanoparticles together with the barrier effect of the clay layers may contribute to greater optimisation of release profiles thus minimising exposure to consumers and the environment. The potential environmental and human toxicity of silver is addressed elsewhere (Tolaymat *et al*., 2010; Han *et al*., 2011; Levard *et al*., 2012) though it is certain that all forms need to be considered given their diverse and inter-connected reactivity; they are all subject to dissolution, precipitation and aggregation.

The safety concerns associated with silver based products will continue until greater awareness and proper control are provided by future research. The antimicrobial coating developed herein is suited to both food and non-food contact packaging (e.g. medical supplies). Its specific use in the former is a definite challenge even though the materials prepared herein are likely to conform to specified migration limits for Ag^+. Moreover, they could be utilised to protect biodegradable materials since these can undergo attack from microbes, especially when stored at relatively high temperatures and humidity.

5. Conclusions

The preparation and use of silver clays as antimicrobial agents and water vapour barrier enhancers in starch-plasticiser-clay based coatings has been assessed. The prewashing of the clay mineral significantly reduced the production of insoluble silver complexes such as AgCl, $AgCO_3$ or $AgSO_4$ by avoiding the reaction of extraneous salts with silver nitrate. Silver exchanged clay was successfully prepared, but not in the complete absence of insoluble silver complexes. These combinations of different silver species supported on the clay substrate have the potential to offer a dynamic mechanism for sustained release.

The silver clays showed potent antimicrobial activity towards the *E.coli, K. rhizophila* and *A. niger*. The lowest concentration of silver-clay assessed (0.03 wt%) still exhibited a strong antimicrobial affect towards *E. coli*. Silver oxide also exhibited strong antimicrobial activity.

The dispersion of silver clays in the coatings was demonstrated, using XRD, to be comparable to that of sodium clay. Water vapour barrier properties of coatings containing silver clays were largely unaffected.

ACKNOWLEDGMENT: The work was conducted within the Project FLEXPAKRENEW (NMP3-SL-2008-207810) which was financed by the 7th Framework Programme of the European Union.

References

Benhacine, F., Hadj-Hamou, A.S., Habi, A., 2016. Development of long-term antimicrobial poly(ε-caprolactone)/silver exchanged montmorillonite nanocomposite films with silver ion release property for active packaging use. Polym. Bull., 73, 1207-1227.

Busolo, M., Fernandez, P., Ocio, M.J., Laragon, J.M., 2010. Novel silver-based nanoclay as an antimicrobial in polylactic acid food packaging coatings. Food Addit. Contam. 27, 1617-1626.

Dizman, B., Badger, J.C., Elasri, M.O., Mathias, L.J., 2007. Antibacterial fluoromicas: a novel delivery medium, Appl. Clay Sci. 38, 57-63.

Dong, Y., Ma, Y., Zhai, T., Shen, F., Zeng, Y., Fu, H., Yao, J., 2007. Silver nanoparticles stabilized by thermoresponsive microgel particles: synthesis and evidence of an electron donor-acceptor effect, Macromol. Rapid Commun., 28 2339-2345.

Han, W., Yu, Y.J., Li, N.T., Wang, L.B., 2011. Application and safety assessment for nano-composite materials in food packaging, Chin. Sci. Bull., 56, 1216-1225.

Herrera, M., Carrion, P., Baca, P., Liebana, J., Castillo, A., 2001. In vitro antibacterial activity of glass-ionomer cements, Microbios, 104, 141.

Huang, H., Yang, Y., 2008. Preparation of silver nanoparticles in inorganic suspensions, Compos. Sci. Technol., 68, 2948-2953.

Johansson, C., Bra, J., Mondragon, I., Nechita, P., Plackett, D., Simon, P., Svetec, D.G., Virtanen, S., Baschetti, M.G., Breen, C., Clegg, F., Aucejo, S., 2012. Renewable Fibres and Biobased Materials for Packaging applications - A review of recent developments, Bioresources, 7, 2506-2552.

Jones, S.A., Bowler, P.G., Walker, M., Parsons, D., 2004. Controlling wound bioburden with a novel silver-containing Hydrofiber((R)) dressing, Wound Repair Regen., 12, 288- 94.

Keller-Besrest, F., Benazeth, S., Souleau, C., 1995. EXAFS structural investigation of a silver-added montmorillonite clay, Mater. Lett. 24, 17-21.

Levard, C., Hotze, E.M., Lowry, G.V., Brown, G.E., 2012. Environmental transformations of silver nanoparticles: impact on stability and toxicity, Environ. Sci. Technol. 46, 6900-6914.

Magana, S.M., Quintana, P., Aguilar, D.H., Toledo, J.A., Angeles-Chavez, C., Cortes, M.A., Leon, L., Freile-Pelegrin, Y., Lopez, T., Torres Sanchez, R.M., 2008. Antibacterial activity of montmorillonite modified with silver, J. Mol. Catal. A: Chem. 281, 192-199.

Marambio-Jones, C., Hoek, E.M.V., 2010. A review of the antibacterial effects of silver nanomaterials and potential implications for human health and the environment, J. Nanopart. Res. 12, 531-1551.

Miyoshi, H., Ohno, H., Sakai, K., Okamura, N., Kourai, H., 2010 Characterisation and photochemical and antibacterial properties of highly stable silver nanoparticles prepared on montmorillonite clay in n-hexanol, J. Colloid Interface. Sci., 345, 433-441.

Moretro, T., Langsrud, S., 2011. Effects of Materials Containing Antimicrobial Compounds on Food Hygiene, J. Food. Protection, 74, 1200-1211.

Mthombeni, N.H., Mpenyana-Monyatsi, L., Onyango, M.S., Momba, M.N.B., 2012. Breakthrough analysis for water disinfection using silver nanoparticles coated resin beads in fixed-bed column, J. Hazard. Mater., 217, 133-140.

Nikolov, P., Genov, K., Konova, P., Milenova, K., Batakliev, T., Georgiev, V., Kumar, N., Sarker, D.K., Pishev, D., Rakovsky, S., 2010. Ozone decomposition on Ag/SiO_2 and Ag/clinoptilolite catalysts at ambient temperature, J. Hazard. Mater., 184, 16-19.

Ohashi, F., Oya, A., Duclaux, L., Beguin, F., 1998. Structural model calculation of antimicrobial and antifungal agents derived from clay minerals, Appl. Clay Sci. 12, 435-445.

Olsson, E., Johansson, C., Larsson, J., Jarnstrom, L., 2014a Montmorillonite for starch-based barrier dispersion coating – Part 1: The influence of citric acid and poly(ethylene glycol) on viscosity and barrier properties, Appl. Clay Sci., 97-98, 160-166.

Olsson, E., Johansson, C., Larsson, J., Jarnstrom, L., 2014b Montmorillonite for starch-based barrier dispersion coating – Part 2: Pilot trials and PE-lamination, Appl. Clay Sci., 97-98, 167-173.

Pal, T., Sau, T.K., Jana, N.R., 1998. Silver Hydrosol, organosol, and reverse micelle-stabilized sol – a comparative study, J. Colloid Interface Sci., 202, 30-36.

Patakfalvi, R., Dekany, I., 2004. Synthesis and intercalation of silver nanoparticles in kaolinite/DMSO complexes, Appl. Clay Sci. 25, 149-159.

Patel, H.A., Bajaj, H.C., Jasra, R.V., 2009. Synthesis of highly dispersed gold and silver nanoparticles anchored on surfactant intercalated montmorillonite, J. Nanosci. Nanotechnol., 9, 5946-5952.

Praus, P., Turicova, M., Valaskova, M., 2008. Study of silver adsorption on montmorillonite, J. Braz. Chem. Soc., 19, 549-556.

Rai, M.K., Deshmukh, S.D., Ingle, A.P., Gade, A.K., 2012. Silver nanoparticles: the powerful nanoweapon against multidrug-resistant bacteria, J. Appl. Microbiol., 112, 841-852.

Roy, A., Butola, B.S., Joshi, M., 2017. Synthesis, characterization and antibacterial properties of novel nano-silver loaded acid activated montmorillonite. Appl. Clay Sci., 146, 278-285.

Sedlarik, V., Galya, T., Sedlarikova, J., Valasek, P., Saha, P., 2010. The effect of preparation temperature on the mechanical and antibacterial properties of poly(vinyl alcohol)/silver nitrate films, Polym. Degrad. Stab., 95, 399-404.

Schierholz, J.M., Beuth, J., Pulverer, G., 1999. Silver coating of medical devices for catheter-associated infections, Am. J. Med., 107, 101-102.

Seo, Y.I., Hong, K.H., Kim, S.H., Chang, D., Lee, K.H., Kim, Y.D., 2012. Removal of bacterial pathogen from wastewater using Al filter with Ag-containing nanocomposite film by in situ dispersion involving polyol process, J. Hazard. Mater., 227, 469-473.

Shameli, K., Ahmad, M.B., Yunus, W.Z.W., Ibrahim, N.A., Darroudi, M., 2010a. Synthesis and characterisation of silver/talc nanocomposites using the wet chemical reduction method, Int. J. Nanomed., 5, 743-751.

Shameli, K., Ahmad, M.B., Yunus, W.Z.W., Rustaiyan, A., Ibrahim, N.A., Zargar, M., Abdollahi, Y., 2010b. Green synthesis of silver/montmorillonite/chitosan bionanocomposites using the UV irradiation method and evaluation of antibacterial activity, Int. J. Nanomed., 5, 875-887.

Sohrabnezhad, S., Pourahmad, A., Moghaddam, J.M.M., Sadeghi, A., 2015. Study of antibacterial activity of Ag and Ag_2CO_3 nanoparticles stabilized over montmorillonite. Spectrochim. Acta Mol. Biomol. Spectrosc., 136, 1728-1733.

Sondi, I., Salopek-Sondi, B., 2004. Silver nanoparticles as antimicrobial agent: a case on E. coli as a model for Gram-negative bacteria, J. Colloid Interface Sci., 275, 177-182.

Tathdil, I., Sokmen, M., Breen, C., Clegg, F., Kurtulus, C., Bacaksiz, B.E., 2011. Degradation of Candida albicans on TiO_2 and Ag-TiO_2 thin films prepared by sol–gel and nanosuspensions, J. Sol-Gel Sci. Technol., 60, 23-32.

Tokarsky, J., Caokova, P., Rafaja, D., Klemm, V., Valaskova, J., Tomasek, V., 2010. Adhesion of silver nanoparticles on the clay substrates; modelling and experiment, Appl. Surf. Sci., 256, 2841-2848.

Tolaymat, T.M., El Badawy, A.M., Genaidy, A., Scheckel, K.G., Luxton, T.P., Suidan, M., 2010. An evidence based environmental perspective of manufactured silver nanoparticles in syntheses and applications: A systematic review and critical appraisal of peer-reviewed scientific papers, Sci. Total Environ., 408, 999-1006.

Top, A., Ulku, S., 2004. Silver, zinc and copper exchange in a Na-clinoptilolite and resulting effect on antibacterial activity, Appl. Clay Sci. 27, 13-19.

Waterhouse, G.I.N., Bowmaker, G.A., Metson, J.B., 2001. The thermal decomposition of silver (I, II) oxide: a combined XRD, FTIR and Raman spectroscopic study, Phys. Chem. Chem Phys., 3, 3838-3845.

Valaskova, M., Hundakova, M., Kutlakova, K.M., Seidlerova, J., Capkova, P., Pazdziora, E., Matejova, K., Hermanek, M., Klemm, V., Rafaja, D., 2010. Preparation and characterisation of antimicrobial silver/vermiculites and silver montmorillonites, Geochim. Cosmochim. Acta, 74, 6287-6300.

Varadwaj, G.B.B., Parida, K.M., 2013. Montmorillonite supported metal nanoparticles: an update on synthesis and applications. RSC Advances, 3, 13583-13593.

Xiu, A.M., Zhang, Q.B., Puppala, H.L., Colvin, V.L., Alvarez, P.J.J., 2012. Negligible particle-specific antibacterial activity of silver nanoparticles, Nano Lett., 12, 4271-4275.

Yang, X., Yang, L., Wang, X., Yang, F., 2008. Excellent antimicrobial properties of mesoporous anatase TiO_2 and Ag/TiO_2 composite films, Microporous Mesoporous Mater., 114, 431-439.

Yonezawa, T., Onoue, S.Y., Kimizuka, N., 2000. Preparation of highly positively charged silver nanoballs and their stability, Langmuir 16, 5218-5220.

Yoon, K.Y., Byeon, J.H., Park, C.W., Hwang, J., 2008. Antimicrobial effect of silver particles on bacterial contamination of activated carbon fibres, Environ. Sci. Technol., 42, 1251-1255.

Zhao, D., Zhou, J., Liu, N., 2006. Preparation and characterisation of Mingguang palygorskite supported with silver and copper for antibacterial behaviour, Appl. Clay Sci., 33, 161-170.

Figure Captions

Table 1: XRF analysis of silver/sodium bentonites. Weight percent oxide values (top section) and amounts of Ag or Na as a percentage of the clays total CEC value (bottom section), which are based on 100% of the CEC being equal to 2.66 wt% Na_2O (i.e. that present in the PW-Na^+Mt sample).

Figure 1: XRD patterns of fresh powdered a) UW-Na^+Mt, b) PW-Na^+Mt-20%Ag, c) UW-Na^+Mt-20%Ag, d) UW-Na^+Mt-120%Ag and e) UW-Na^+Mt-400%Ag. Symbols represent selected reflections positions for AgCl (•), Ag_2SO_4 (□), Ag_2CO_3 (Δ) and AgO (*).

Figure 2: XRD patterns of fresh powdered UW-Na^+Mt-120%Ag before and after backwashing with NaCl, HNO_3, NaOH and $NaNO_3$. Symbols represent selected reflection positions for AgCl (•), Ag_2SO_4 (□), Ag_2CO_3 (Δ), Ag_2O (○), AgO (*) and metallic silver (+).

Figure 3: TEM micrographs obtained from PW-Na^+Mt-20%Ag.

Figure 4: Antimicrobial results from A) silver-clays (5.7 wt% loading) against *E. coli*, B) PW-Na^+Mt-20%Ag (0.28 wt%) against *A. niger* and C) UW-Na^+Mt-400%Ag (1.4-4.3 wt%) against *K. rhizophila*. A) and B) were present in starch (S1)/PEG600/PW-Na^+Mt coating on glass slides, whereas C) was present in starch (S2)/PEG600/PW-Na^+Mt coating on paper.

Figure 5: Antimicrobial efficacy test results from PW-Na^+Mt-20%Ag against *E. coli* when present in starch (S1)/PEG600/PW-Na^+Mt coatings on glass slides.

Figure 6: Antimicrobial test results from Ag_2O against *E. coli* when present in starch (S1)/PEG600/PW-Na^+Mt coatings on glass slides.

Figure 7: Concentrations of Ag salt in solution determined by ICP-OES after treatment of 0.33 wt% PW-Na^+Mt-20%Ag aqueous dispersions with HNO_3 or $NaNO_3$.

Figure 8: WVTR results from double-layered starch (S1)/PEG600/silver clay coatings on paper substrate. All coatings contain 5.7 wt% silver clay with the exception of the UW-Na^{+}Mt-120%Ag-BW(NaCl)* which contains 28.6 wt%.

Figure 9: XRD patterns of a) powdered PW-20%AgC, b) UW-Na^{+}Mt dispersed in starch (S1) and PEG600, and c) PW-Na^{+}Mt-20%Ag dispersed in starch (S1) and PEG600.

Table 1: XRF analysis of silver/sodium bentonites. Weight percent oxide values (top section) and amounts of Ag or Na as a percentage of the clays total CEC value (bottom section), which are based on 100% of the CEC being equal to 2.66 wt% Na_2O (i.e. that present in the PW-Na^+Mt sample).

wt% Oxide	Silver/Sodium Bentonites						
	UW-Na^+Mt	PW-Na^+Mt	PW-Na^+Mt-20%Ag	UW-Na^+Mt-20%Ag	UW-Na^+Mt-120%Ag	UW-Na^+Mt-120%Ag-BW(NaCl)	UW-Na^+Mt-400%Ag
SiO_2	64.73	66.30	66.12	65.93	67.56	66.97	68.57
Al_2O_3	22.42	23.61	22.67	22.89	23.25	22.72	22.76
Ag_2O	-	-	0.69	1.15	7.43	6.23	15.04
Na_2O	3.18	2.66	2.52	2.53	1.78	2.60	0.62
Cl	0.36	0.00	0.00	0.14	0.33	1.07	0.33
S	0.24	0.00	0.00	0.00	0.02	0.00	0.03
Amounts of Ag or Na (%) relative to total CEC							
Ag			7.0	11.7	75.3	62.7	152.4
Na	119.5	100	94.7	95.1	66.9	97.7	23.3
Total	119.5	100	101.7	106.8	142.2	160.4	175.7

Figure 1: XRD patterns of fresh powdered a) UW-Na^+Mt, b) PW-Na^+Mt-20%Ag, c) UW-Na^+Mt-20%Ag, d) UW-Na^+Mt-120%Ag and e) UW-Na^+Mt-400%Ag. Symbols represent selected reflection positions for AgCl (•), Ag_2SO_4 (□), Ag_2CO_3 (Δ) and AgO (*).

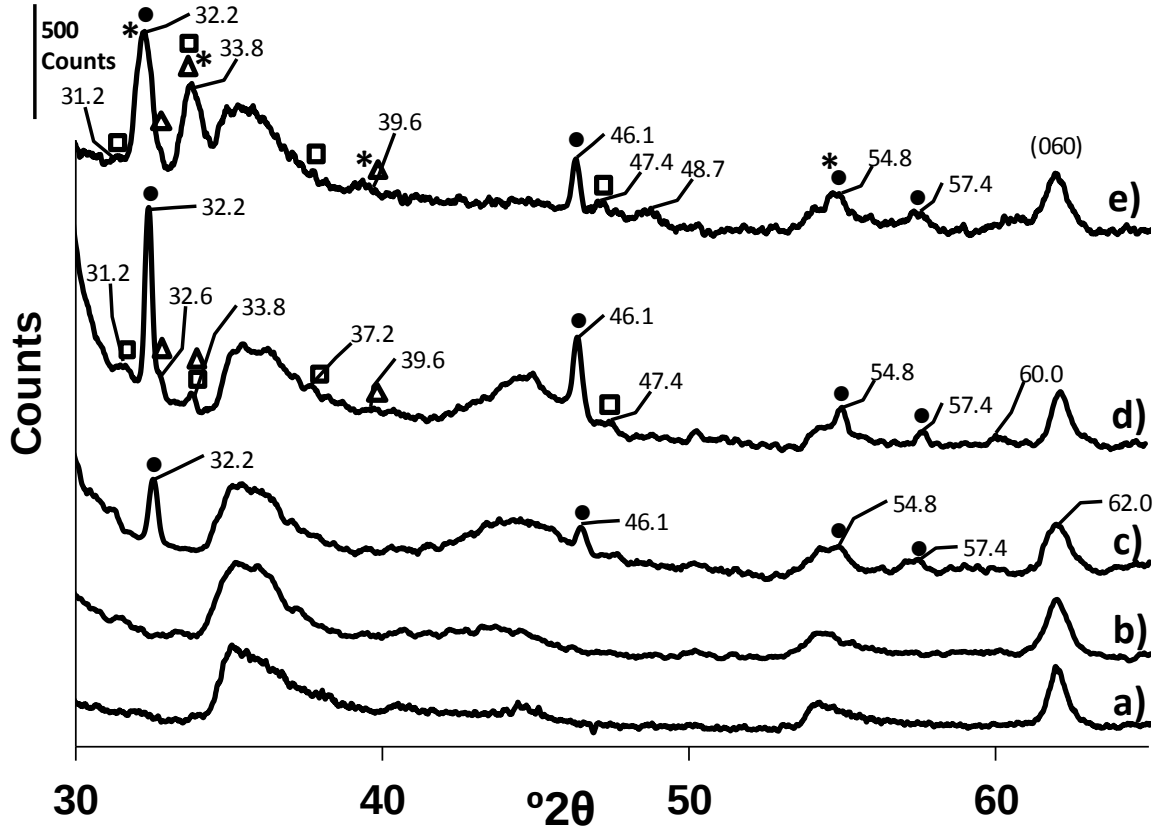

Figure 2: XRD patterns of fresh powdered UW-Na^{+}Mt-120%Ag before and after backwashing with NaCl, HNO_3, NaOH and $NaNO_3$. Symbols represent selected reflection positions for AgCl (•), Ag_2SO_4 (□), Ag_2CO_3 (Δ), Ag_2O (○), AgO (*) and metallic silver (+).

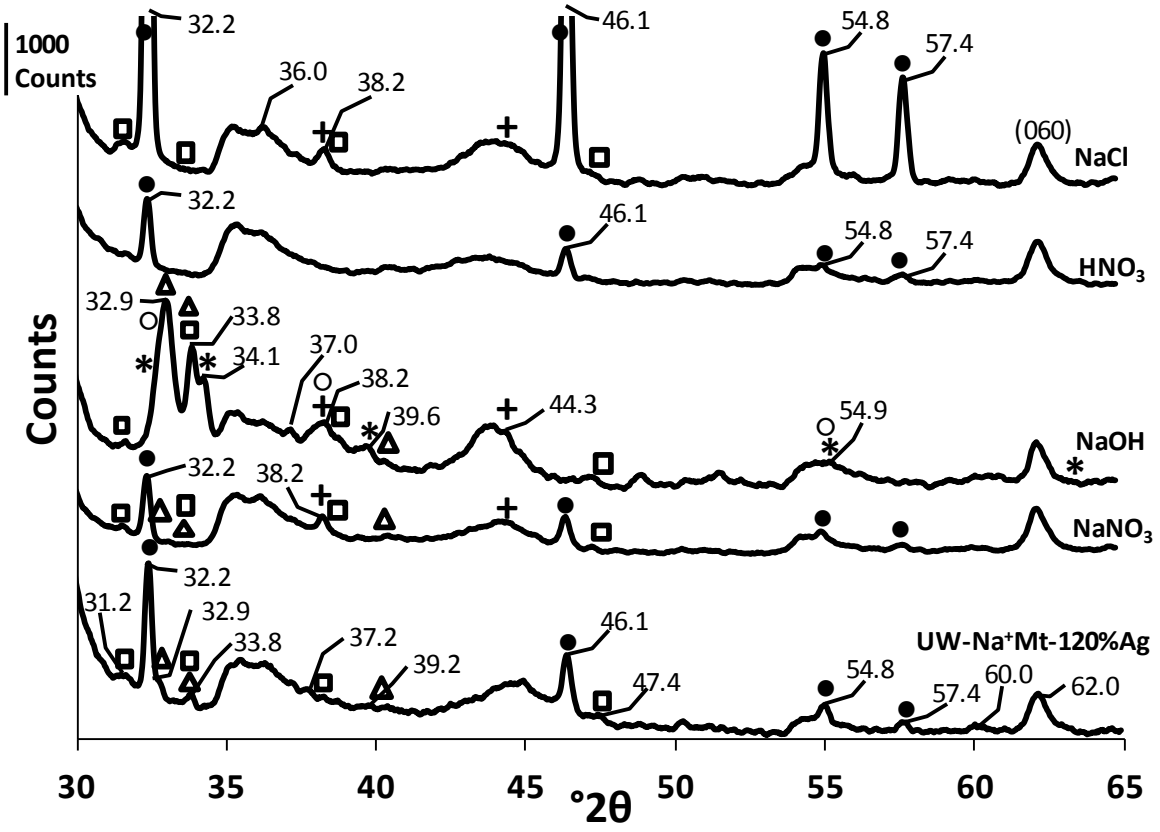

Figure 3: TEM micrographs obtained from PW-Na^{+}Mt-20%Ag.

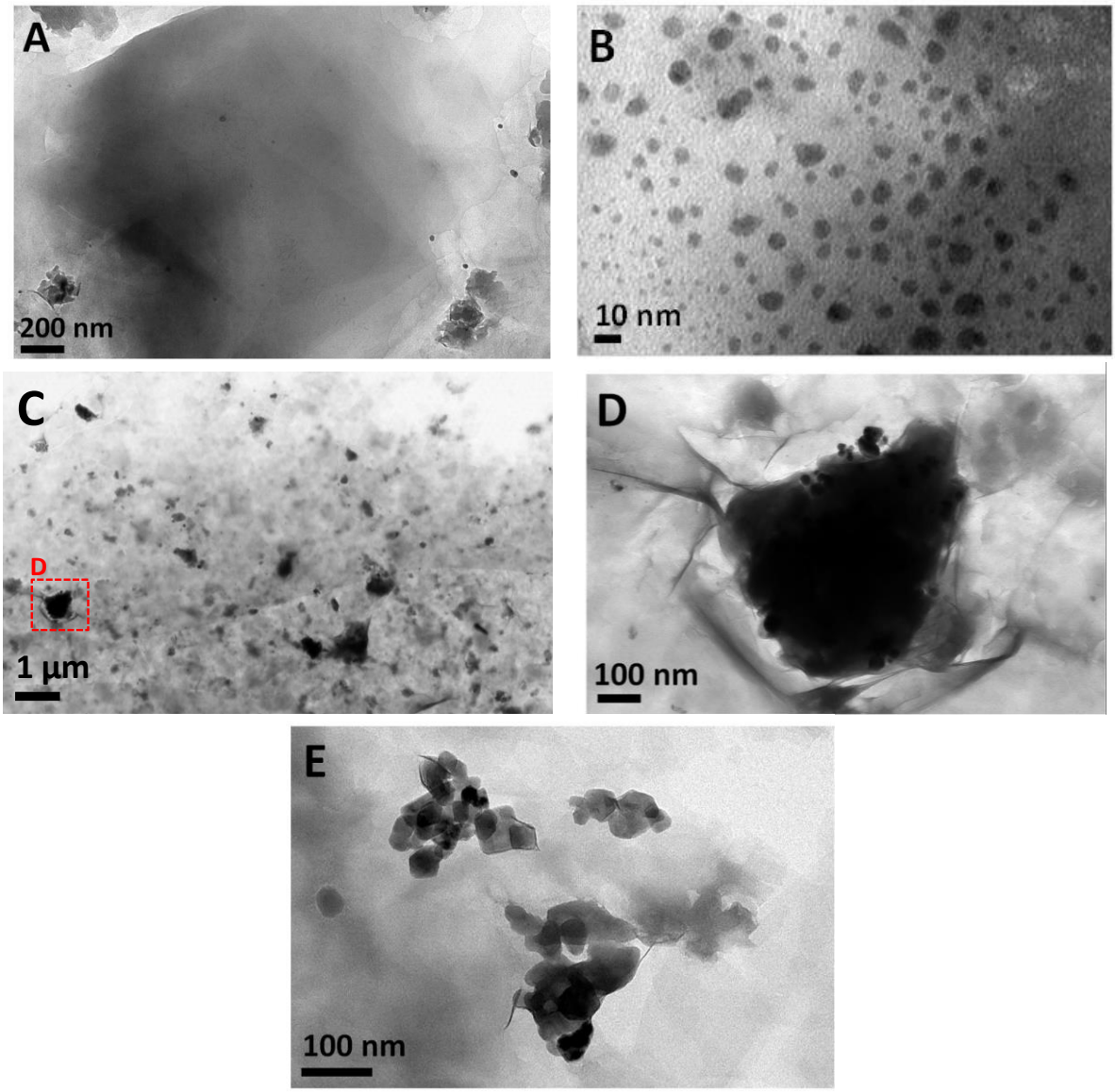

Figure 4: Antimicrobial results from A) silver-clays (5.7 wt% loading) against *E. coli*, B) PW-Na^+Mt-20%Ag (0.28 wt%) against *A. niger* and C) UW-Na^+Mt-400%Ag (1.4-4.3 wt%) against *K. rhizophila*. A) and B) were present in starch (S1)/PEG600/PW-Na^+Mt coating on glass slides, whereas C) was present in starch (S2)/PEG600/PW-Na^+Mt coating on paper.

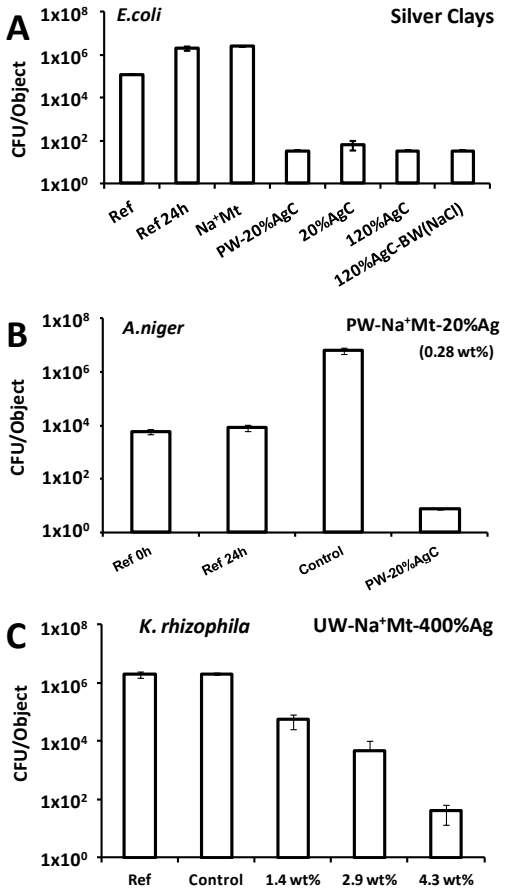

Figure 5: Antimicrobial efficacy test results from PW-Na^+Mt-20%Ag against *E. coli* when present in starch (S1)/PEG600/PW-Na^+Mt coatings on glass slides.

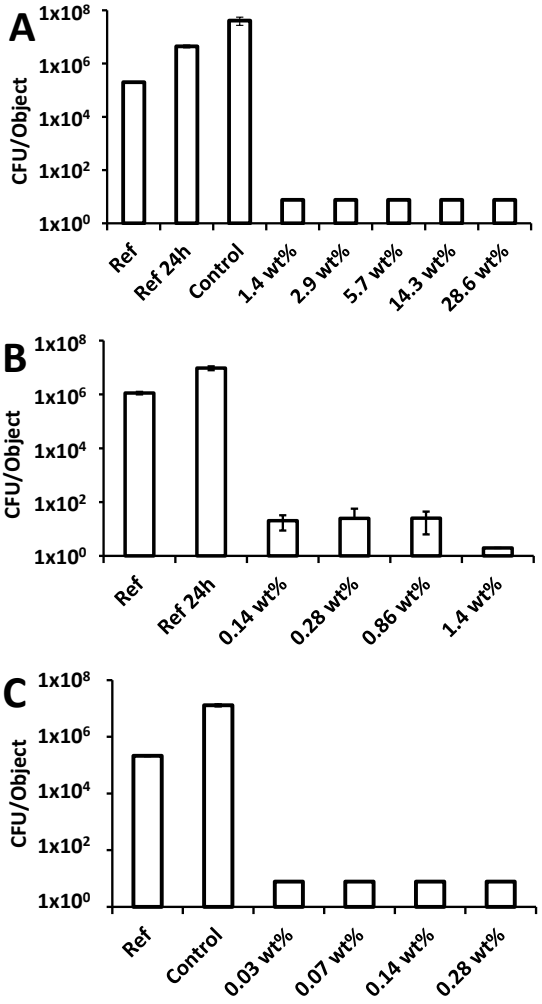

Figure 6: Antimicrobial test results from Ag_2O against *E. coli* when present in starch (S1)/PEG600/PW-Na^+Mt coatings on glass slides.

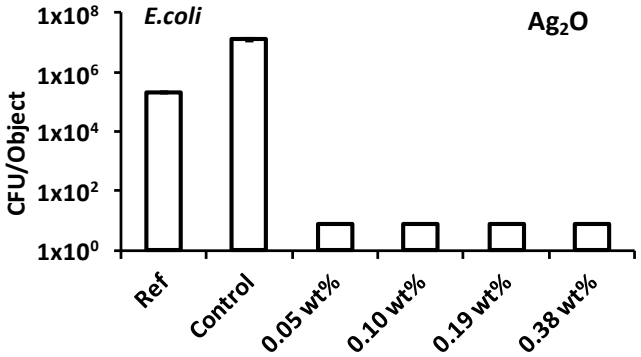

Figure 7: Concentrations of Ag salt in solution determined by ICP-OES after treatment of 0.33 wt% PW-Na^+Mt-20%Ag aqueous dispersions with HNO_3 or $NaNO_3$.

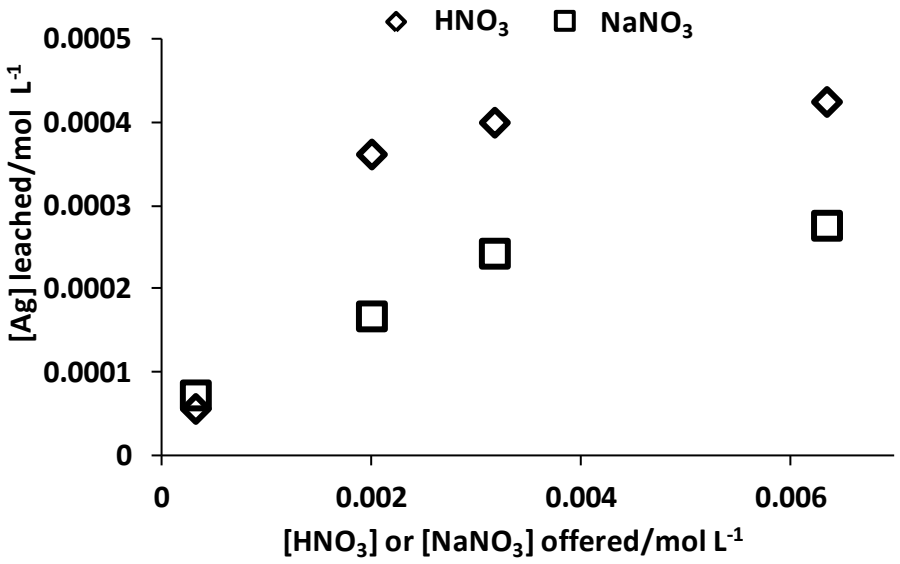

Figure 8: WVTR results from double-layered starch (S1)/PEG600/silver clay coatings on paper substrate. All coatings contain 5.7 wt% silver clay with the exception of the UW-Na^+Mt-120%Ag-BW(NaCl)* which contains 28.6 wt%.

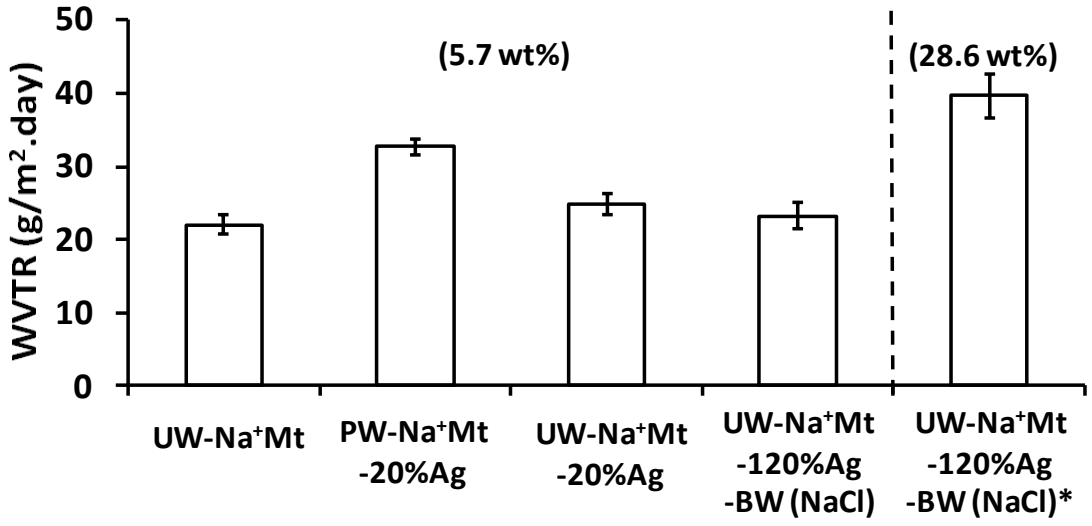

Figure 9: XRD patterns of a) powdered PW-20%AgC, b) UW-Na^{+}Mt dispersed in starch (S1) and PEG600, and c) PW-Na^{+}Mt-20%Ag dispersed in starch (S1) and PEG600.